LUND UNIVERSITY

Deubiquitinating activity of CYLD is impaired by SUMOylation in neuroblastoma cells.

Kobayashi, Tamae; Masoumi, Katarzyna; Massoumi, Ramin

Link to publication

Total number of authors:
3

LUND UNIVERSITY

PO Box 117
221 00 Lund
+46 46-222 00 00

Deubiquitinating activity of CYLD is impaired by SUMOylation in neuroblastoma cells

Tamae Kobayashi, Katarzyna Chmielarska Masoumi and Ramin Massoumi

Translational Cancer Research, Department of Laboratory Medicine, Lund University, Medicon Village, Lund, Sweden

Contact:

Ramin Massoumi
Lund University
Molecular Tumor Pathology
Building 404, A3
Scheelevagen 8
22363 Lund, Sweden

Phone: +46768890264
E-mail: Ramin.Massoumi@med.lu.se

Running Title: CYLD SUMOylation regulates differentiation

Abstract

CYLD is a deubiquitinating enzyme that has a pivotal role in modulating NF-κB signaling pathways by removing the lysine 63 and linear-linked ubiquitin chain from substrates such as TRAF2 and TRAF6. Loss of CYLD activity is associated with tumorigenicity and levels of CYLD are lost or downregulated in different types of human tumors. In the present study, we found that high CYLD expression was associated with better overall survival and relapse-free neuroblastoma patient outcome, as well as inversely correlated with the stage of neuroblastoma. Retinoic acid-mediated differentiation of neuroblastoma restored CYLD expression and promoted SUMOylation of CYLD. This post-translational modification inhibited deubiquitinase activity of CYLD against TRAF2 and TRAF6 and facilitated NF-κB signaling. Overexpression of non-SUMOylatable mutant CYLD in neuroblastoma cells reduced retinoic acid-induced NF-κB activation and differentiation of cells, but instead promoted cell death.

Keywords: CYLD; SUMO; neuroblastoma; deubiquitinating enzyme

Introduction

Neuroblastoma is the most common extracranial tumor in children, accounting for 15% of childhood cancer deaths (1, 2). Neuroblastoma originates from the sympathetic nervous system and is composed of undifferentiated and poorly differentiated neuroblasts arising from the different stages of sympathoadrenal lineage of neural crest origin (3-6). Earlier reports identify that in neuroblastoma expression of markers that are upregulated in later stages of the neuronal lineage of sympathetic nervous system differentiation, such as neurotrophic tyrosine kinase, receptor, type 1 (*NTRK1)* and growth associated protein 43 (*GAP43)* is indicative of better prognosis (7, 8). The age of patient, genetic aberrations (*N-MYC* amplification and deletion of chromosome 11 q), and metastatic spread are important factors with regard to treatment decision and patient prognosis. The International Neuroblastoma Staging System (INSS) is divided into 1-4 stage groups and stage 4S, which has the ability to spontaneously regress (4, 9). Patients older than 1 ½ years with Stage 4 disease have the worse prognosis, with an overall survival of < 50% (3).

Surgery, chemotherapy, radiotherapy, and high-dose chemotherapy with autologous stem cell transplantation are commonly used as treatment therapy for neuroblastoma patients. In addition, terminal differentiation of neuroblastoma cells induced by retinoids is used as a current standard therapy for high-risk neuroblastomas in order to eliminate residual tumor cells that are resistant after intensive chemotherapy and stem cell transplantation (1, 10-12). Retinoids act on upregulating diverse sets of differentiation-related gene expression via retinoic acid receptors (RAR and RXR) such as *GAP43* and neurotrophin receptors (*TrK*) (13-15). In addition, retinoids

can also downregulate expression of certain genes such as *N-MYC*, concurrent with the arrest of cell proliferation (12, 16, 17). Elucidating the mechanisms behind the differentiation of neuroblastoma cells is therefore of clinical importance.

CYLD mutation was originally discovered in patients developing familial cylindromatosis, which is a benign tumor of skin appendages (18). Loss of CYLD expression has also been found in many different tumors (19), however, the function of CYLD in neuroblastoma is unknown. CYLD is a deubiquitinating enzyme that cleaves lysine 63 and linear linked polyubiquitin chains from the substrates (20, 21). Many of the known deubiquitinating substrates for CYLD include components of nuclear factor kappa B (NF-κB) signaling such as tumor necrosis factor receptor-associated factor 2 (TRAF2), tumor necrosis factor receptor-associated factor 6 (TRAF6), NF-κB essential modifier (NEMO, also named IKKγ), and B cell lymphoma 3 (BCL3) (22-25), thus, affecting the downstream signaling pathway. As many reports highlight the importance of CYLD expression, the regulatory mechanism of CYLD at the protein level and its influence on cellular activity and signaling remains largely unknown.

In the present study we were able to identify post-translational modification of CYLD by Small Ubiquitin-Related Modifier (SUMO) upon all-trans-retinoic acid (ATRA)-induced neuroblastoma differentiation. This post-translation modification resulted in reduced deubiquitinase activity of CYLD against its target substrates, including TRAF2 and TRAF6 and modification of NF-κB signaling.

Results

CYLD expression is associated with clinical outcomes in neuroblastoma patients

In order to investigate whether CYLD expression is altered in neuroblastoma, we studied the association of CYLD levels with neuroblastoma patient outcomes. A Kaplan-Meier survival analysis using a microarray data set from 88 neuroblastoma patients (26) revealed that high CYLD expression was associated with better overall survival (Figure 1A) and relapse-free neuroblastoma patient outcomes (Figure 1B). Furthermore, the relative expression level of CYLD was inversely correlated with tumor stage using the International Neuroblastoma Staging System (INSS) (Figure 1C). Oncogene *N-MYC* is often amplified in aggressive and undifferentiated neuroblastomas and its expression correlates with advanced disease (27-29). Analysis of *N-MYC* amplification in neuroblastoma patients showed that CYLD expression was significantly lower in *N-MYC* amplified, compared to non-amplified, neuroblastomas (Figure 1D). We could not find any correlation of CYLD expression with the different cellular phenotypic variants of neuroblastoma cell lines including neuroblastic (N-type; SK-N-F1, SK-N-RA, SH-SY5Y and IMR-32) or more malignant neuroblastoma cells, the intermediate type (I-type; SK-N-BE(2)C and LA-N-2). Instead, it appeared that cell lines with the lowest expression level of CYLD tend to be either multidrug resistant or derived from a patient after therapy (Figure 1E and 1F).

All-trans-retinoic acid (ATRA)-treatment increases NF-κB activation

Since we found a negative correlation between CYLD and N-MYC expression (see Fig. 1D), this led us to hypothesize that CYLD expression could be regulated upon differentiation of neuroblastoma. To test this hypothesis, we treated the SK-N-BE(2)C cell line with all-trans retinoic acid (ATRA). We chose to use the SK-N-BE(2)C cell line, since this cell line expresses low levels of CYLD (see Figure 1E and 1F) and is highly aggressive and multidrug resistant, but still has the capacity to differentiate into neuron-like cells in response to ATRA treatment. Figure 2A and 2B shows ATRA-mediated cell differentiation evaluated by changes in cell morphology including neurite outgrowth and downregulation of N-MYC in SK-N-BE(2)C cells. This effect was reversible by removal of ATRA and replacing it with DMSO (Figure 2A, ATRA→DMSO). One of the ATRA-mediated signaling pathways is the activation of the transcription factor, NF-κB (30-32). Consistent with these reports, the NF-κB repressor protein, inhibitor of NF-κB (IκB α) level was decreased during ATRA-induced neuroblastoma treatment, and returned to normal levels when ATRA was replaced with DMSO (Figure 2C). This observation was supported by NF-κB luciferase assay, where an increase in κB promoter activity upon ATRA-treatment compared with DMSO-treated cells was observed (Figure 2D). The ATRA-mediated NF-κB activation was transient, as after 8-10 days, we could see downregulation of NF-κB promoter activity (Figure 2E). Prolonged stimulation with ATRA (8-10 days) also led to an increase in cell death (Figure 2F). These results suggest that short time stimulation with ATRA increases NF-κB signaling and promotes differentiation of cells, while prolonged ATRA stimulation reduces NF-κB activation and mediates cell death.

CYLD is SUMOylated upon all-trans-retinoic acid (ATRA)-treatment

Next, we investigated whether stimulation of neuroblastoma cells with ATRA can affect CYLD expression. RT-qPCR and Western Blot analyses showed a significant upregulation of CYLD gene expression in response to ATRA, which was reversible after ATRA removal (Figure 3A and 3B). At the protein level, after 3-6 days, we observed a slow migrating band in cells treated with ATRA, corresponding to a post-translational modified form of CYLD (Figure 3B). This slow migrating band was lost when the ATRA was removed (Figure 3C). Since one of the post-translational modifiers that promotes cellular differentiation is SUMOylation (33, 34), we studied whether ATRA can alter the overall levels of SUMOylated proteins. An increase in the total levels of SUMO1- and SUMO2/3-modified proteins in cells treated with ATRA was observed. However, this effect was reversible when the medium was replaced from ATRA to DMSO (Figure 3D). To investigate whether endogenous CYLD is SUMOylated during ATRA-induced neuroblastoma differentiation, SK-N-BE(2)C neuroblastoma cells were treated with ATRA for 3 and 6 days and the lysates were used for immunoprecipitation with CYLD antibody. Figure 3E shows the association of SUMO with CYLD in the presence of ATRA. The reciprocal immunoprecipitation with SUMO1 or SUMO2/3 antibodies using 8M urea treated lysates confirmed SUMOylation of CYLD upon ATRA treatment (Figure 3F). Moreover, we found that SUMOylation of CYLD is transient. Treatment of SK-N-BE(2)C neuroblastoma cells with ATRA reduced association of SUMO with CYLD after 8 days, and SUMOylation of CYLD was completely undetected after 10 days without any changes in the total levels of CYLD (Figure 3G). The post-translational modification of CYLD by SUMO1 and SUMO2 was further confirmed by performing *in vitro* SUMOylation assay (Figure 4A) as well as in cells overexpressing Flag-tagged full length CYLD and SUMO1 (Figure 4B). To determine the region responsible for binding to SUMO, we generated a series of CYLD deletion mutants. As shown in Supplementary figure 1, only CYLD 1-212 (aa 1-212) was strongly post modified in this assay.

Next, we used purified CYLD 1-212 in an *in vitro* SUMOylation assay and could show that N-terminal part of CYLD contain SUMO acceptor site (Figure 4C) for both SUMO1 and SUMO2. More specifically, lysine 40 was identified as a potential SUMO-binding site in the short fragment of CYLD protein (CYLD 1-212) using the SUMO predictor program (SUMOplot™ Analysis Program: http://www.abgent.com/sumoplot, Figure S2). This sequence is highly conserved between the human, rat, mouse, bovine, chicken, and chimpanzee (Figure S3). Furthermore, mutation analysis (K40R) of this site in CYLD 1-212 (Figure 4D) or full length CYLD construct (Figure 4E) abolished SUMOylation.

Deubiquitinase activity of CYLD is modulated by SUMOylation

Seeking an explanation for CYLD SUMOylation in ATRA-stimulated neuroblastoma cells, we analyzed stability, subcellular translocation, substrate affinity changes, and deubiquitinating (DUB) activity of CYLD. We could not see any differences in the stability of full length and CYLD SUMO mutant (CYLD-K40R) by the treatment of cells with MG132, an inhibitor of 26S proteasome dependent protein degradation (Figure 5A). Direct visualization of EGFP-CYLD and EGFP-CYLD-K40R mutant using confocal microscopy showed that both wildtype and SUMO-mutant CYLD are mainly localized in the cytoplasm of cells (Figure 5B). No differences could be observed in the substrate binding capacity between wildtype and CYLD-K40R to TRAF2 or TRAF6 (Figure 5C). *In vitro* DUB assay demonstrated that SUMOylation of CYLD reduces DUB activity of wildtype CYLD, whereas non-SUMOylable CYLD (CYLD-K40R) could de-conjugate lysine 63 chains (Figure 5D). Furthermore, the deubiquitinating activity of wildtype CYLD toward TRAF6 ubiquitination was reduced when the cells were co-expressing His-SUMO1 or His-SUMO2 (Figure 5E and 5F). However, co-expression of non-SUMOylable full

length CYLD (CYLD-K40R) and SUMO, reduced lysine 63-linked polyubiquitin conjugation to TRAF6 (Figure 5E and 5F). This effect was not limited to TRAF6, since deconjugation of ubiquitin chains from TRAF2 was also dependent on the CYLD SUMOylation (Figure 5G). To further confirm that the deubiquitinating activity of CYLD against its substrates is reduced due to SUMOylation, cells were transfected with TRAF2, full length or CYLD-K40R and ubiquitin in the presence or absence of SUMO constructs. Figure 5H shows that in the absence of SUMO (Lanes 5 and 7) the effect of overexpression of wildtype CYLD and CYLD-K40R on cleavage of the lysine 63 linked ubiquitin of TRAF2 was similar (Figure 5H). However, expression of SUMO together with wildtype CYLD prevented deubiquitination of TRAF2 to the same levels as in the control (Lanes 3 and 4). In contrast, CYLD-K40R unconjugated ubiquitin from TRAF2, both in the presence and absence of SUMO construct (Lanes 6 and 7). These results suggest that deubiquitin activation of CYLD is modulated by SUMOylation.

To test the effect of CYLD SUMOylation in ATRA-mediated NF-κB activation, we transfected SK-N-BE(2)C neuroblastoma cells with wildtype and CYLD-K40R and performed NF-κB promoter luciferase activity. CYLD K40R mutant significantly reduced ATRA-induced-κB promoter activity (Figure 5I) as well as degradation of IκB-α and phosphorylation of p65 (Figure 5J). As expected, overexpression of wildtype CYLD and CYLD-K40R reduced NF-κB promoter activity, degradation of IκB-α, and phosphorylation of p65 compared to mock transfected cells in the absence of ATRA-treatment (Figure S4). The morphological effects of the overexpression of CYLD or CYLD-K40R in the presence of ATRA for one hour were quantified by counting the number of transfected cells with cell processes longer than the length of two cell bodies as an indication of differentiation. In SK-N-BE(2) cells, overexpression of CYLD induced long

processes in 61% of the transfected cells, a substantially higher number than cells expressing EGFP only, where 25% of transfected cells had long processes. Expression of CYLD-K40R resulted in a decreased number of cells with long processes (35%, Figure 5K and Figure S5). Taken together, these results suggest that SUMOylation of CYLD at lysine 40 interferes with CYLD deubiquitinating activity without any alteration in the stability, subcellular translocation or substrate affinity changes. Furthermore, SUMOylation of CYLD in neuroblastoma mediated by ATRA induces NF-κB activation and differentiation via inhibition of CYLD DUB activity (See Figure 5L).

To investigate whether CYLD expression can be correlated with differentiation markers we used a data set from 88 neuroblastoma patients and compared CYLD expression with late sympathetic neuronal differentiation and early neural crest associated genes. As demonstrated in Figure 6 and Table 1, we found strong correlation between CYLD and late sympathetic neuronal differentiation marker genes, such as neurotrophic tyrosine kinase, receptor, type 1 (*NTRK1)*, growth associated protein 43 (*GAP43)*, neuropeptide Y (*NPY*), stathmin-like 2 (*STMN2)*, and B-cell CLL/lymphoma *2 (BCL2)* (Figure 6A and Table1), whereas, two of the early neural crest associated genes, vimentin (*VIM*) and inhibitor of DNA binding 2 (*ID2*) were inversely correlated with CYLD expression (Figure 6B and Table1).

DISCUSSION

Neuroblastoma is a rare childhood cancer that arises from the developing sympathetic nervous system. Many factors including age and stage, as well as the genetic features of the tumor,

determine whether it will spontaneously regress or metastasize and become refractory to therapy. There are multiple studies defining the role of different tumor suppressor genes in the development or progression of neuroblastoma (35). In the present study, we investigated the role of deubiquitination enzyme CYLD in neuroblastomas. Initially, we found that higher CYLD expression in neuroblastoma patient samples correlated with better survival and lower tumor stages. Furthermore, CYLD expression was significantly lower in *N-MYC* amplified, which are prediction markers for poor outcomes in neuroblastoma (28). In addition, low CYLD expression was observed in a subset of neuroblastoma cell lines that are multidrug resistant or derived from relapsed neuroblastoma after intensive chemotherapy. Recently, ATRA has been included to the standard of care for high-risk neuroblastoma (36). Consistent with our findings that *N-MYC* non-amplified patients have significantly higher CYLD expression, ATRA rescues the levels of CYLD in neuroblastoma through the gene transcription mechanism. Furthermore, analyzing microarray data from neuroblastoma patient samples showed that CYLD expression was positively correlated with gene expression of late differentiation markers, including *STMN2, SCG2, NTRK1, BCL2,* and *GAP43*, while neural crest marker genes, including *VIM* and *ID2* were negatively correlated with CYLD expression. In general, the expression of markers that are expressed in later stages of differentiation is an indication of better prognosis (12, 18).

Previous studies identified SUMO as playing a vital role in cell differentiation. Gene encoding proteins involved in SUMOylation are upregulated during Ca^{2+}-induced human keratinocyte cell differentiation and in ATRA-induced acute promyelocytic leukemia cell differentiation (33, 34). In the present study, we found that ATRA-treatment of neuroblastoma cell lines leads to a transient increase in the expression of SUMO1 and SUMO2 proteins. In addition, ATRA also promoted a transient activation of the classical NF-κB signaling pathway including IκB-α

degradation, phosphorylation of p65, and NF-κB promoter activity. The highest activation of NF-κB signaling and neurite outgrowth, which is a sign of neuroblastoma cell differentiation, could be observed between 1-6 days treatment with ATRA. Prolonged stimulation with ATRA (after 6 days), reduced NF-κB signaling and instead facilitated cell death.

ATRA-mediated upregulation of CYLD at the protein level was followed by an immediate post-transcriptional modification of CYLD through the SUMOylation process. However, this effect was transient. Constant CYLD SUMOylation was observed only between 1-6 days, whereas after 8-10 days, as the total level of CYLD protein was unchanged, the SUMOylation of CYLD was reduced. As no changes in protein stability, substrate binding, or localization of CYLD SUMO mutant compared to wildtype CYLD could be observed, reduced DUB activity was identified. Since transient CYLD SUMOylation paralleled NF-κB activation, we investigated whether this post-translational modification could interfere with the NF-κB signaling pathway in ATRA-stimulated neuroblastoma cells. Ubiquitination of TRAF2 and/or TRAF6 is an essential process for NF-κB activation, and direct binding and deubiquitination of TRAF2/6 by CYLD attenuates downstream signaling (37, 38). Here, we could show that SUMOylation of CYLD at lysine 40 prevents removal of the lysine 63 linked polyubiquitin chain from its substrates including TRAF6 and TRAF2. Furthermore, inhibition of CYLD deubiquitinase activity was essential for ATRA-mediated NF-κB signaling and differentiation of neuroblastoma cells, whereas prolonged ATRA treatment led to reduced CYLD SUMOylation, which in turn, prevented NF-κB signaling pathway and promoted cell death. This finding suggests that the balance between non-SUMOylated and SUMOylated CYLD can direct differentiation or cell death by regulating NF-κB signaling in neuroblastoma (See Figure 5L). Indeed, retinoic acid can induce differentiation

and apoptosis of neuroblastoma cells (39, 40). Previously, it has been shown that CYLD promotes apoptosis or necrosis by blocking NF-κB signaling activity (25, 41, 42). In addition, the NF-κB pathway is generally tightly regulated with a negative feedback loop, for instance, by the induction of SUMO protease SENP2 upon genotoxic stress to attenuate cell survival response (43). This raises the possibility that SUMOylation of CYLD could be reversed after initiation of neuroblastoma differentiation by negative feedback loop. This is crucial since CYLD is exclusively localized in cytoplasm, and it has been reported that SUMOylation of extra nuclear protein can have a significant acute effect on neuronal function (44).

In conclusion, our study provides evidence that CYLD expression in neuroblastoma is rescued by ATRA-mediated differentiation of cells and post-translational modification of CYLD via SUMOylation. The SUMOylation of CYLD interferes with its DUB activity, which is vital for directing cell signaling decisions to promote either differentiation or apoptosis.

Materials and methods

Cell culture and neuroblastoma differentiation treatments

SK-N-BE(2)C and SH-SY5Y, human neuroblastoma cells were grown in minimum essential medium (MEM) (Sigma), whereas LA-N-2, SK-N-RA, SK-N-F1 and IMR-32 human neuroblastoma cells were grown in RPMI 1640 medium (Sigma). Hela cells were kept at 37°C in a humidified atmosphere containing 5% CO_2 and 95% air. For induction of neuroblastoma differentiation, SK-N-BE(2)C cells were cultured in MEM with 1% of fetal bovine serum, 100 IU/ml penicillin, 100 µg/µl streptomycin in the presence of 1 or 5 µM all-trans-retinoic acid (ATRA, Sigma-Aldrich) for different time points. Photomicrographs of the cell morphologies were taken with a phase-contrast microscope.

For morphological studies at the end of transfections, cells were fixed in 4% paraformaldehyde in PBS for 10 min and mounted on microscopy slides. The transfected cells were considered to have long processes if the length of the process exceeded that of two cell bodies. At least 200 transfected cells per experiment were counted.

Immunoblotting and immunoprecipitation

For immunoprecipitation studies, cells were washed three times in ice cold PBS and lysed on ice in a RIPA lysis buffer (150 mM NaCl, 1% Triton X-100, 50 mM Tris HCl, pH 7.6, 5 mM EDTA, 0.1% SDS, 1% Na deoxycholate) supplemented with EDTA-free Complete™ protease inhibitor cocktail (Roche), 2.1 mM Na_3VO_4, 0.02 mM Iodoacetamide (Sigma-Aldrich), 20 mM N-ethylmaleimide (Sigma-Aldrich) and 1mM phenylmethylsulfonyl fluoride (Sigma-Aldrich) and lysates were passaged through a 23 gauge syringe. Lysates were cleared by centrifugation at

14,000 x *g* for 10 min at 4°C, and the supernatants were pre-cleared two times with IgG-beads for 60 min prior to IP. The pre-cleared lysates were incubated overnight with 1-2 μg of antibodies followed by incubation with protein G-coupled microbeads for 30 minutes on rotation at 4°C. The immune complexes were recovered by applying the lysates on μColumns placed in the magnetic field of a μMACS Separator. Following washes the complexes were eluted with sample buffer. For denatured condition, lysates containing 8 M urea was used for lysing cells and the lysates were diluted 20 times with lysis buffer without urea prior to IP.

For the immunoblotting process, whole cell lysates were prepared using RIPA buffer with protease inhibitors and were transferred onto the PVDF membranes after being resolved by SDS-PAGE. Membranes were pre-incubated with 5% dried milk in PBS followed by incubation with primary antibodies. The membranes were incubated with the following antibodies: rabbit polyclonal TRAF2 (C-20, Santa Cruz), rabbit polyclonal TRAF6 (H-274, Santa Cruz), rabbit polyclonal HA (Y-11; Santa Cruz), rabbit monoclonal Phospho-NF-κB p65 (serine 536, Cell Signaling, #3033,), rabbit monoclonal NF-κB p65 (4764, Cell Signaling), rabbit polyclonal His (2365, Cell Signaling), rabbit monoclonal K63-linkage specific polyubiquitin (D7A11, Cell Signaling), rabbit monoclonal CYLD (D1A10, Cell Signaling), mouse monoclonal SUMO-1 (21C7, Invitrogen), rabbit polyclonal SUMO1 (PW9460, Enzo Life Sciences), rabbit polyclonal SUMO2/3 (PW9465, Enzo Life Sciences), rabbit polyclonal SUMO2/3 (ab3742, Abcam), mouse monoclonal M2 Flag (F3165; Sigma-Aldrich), and previously generated rabbit polyclonal CYLD (23). Secondary horseradish peroxidase-conjugated antibodies were obtained from GE healthcare and antibodies conjugated to Alexa dyes from Invitrogen. Control IgG were obtained from

Abcam and goat serum used for blocking from Sigma-Aldrich. The chemiluminescence was captured with a charge-coupled device camera (Fujifilm).

Quantitative real time PCR (qRT-PCR)

RNA was isolated using a Perfect Pure RNA cell & Tissue kit (5 PRIME) according to the manufacturer's instructions. First strand cDNA synthesis was performed using a high-capacity cDNA reverse transcription kit (Applied Biosystems) with random primers and 1-2 µg of RNA. Reaction for qRT-PCR was prepared using cDNAs with SYBR$^®$ Green QPCR master mix (Agilent) and qRT-PCR was performed on the Mx3005P real-time thermocycler (Stratagene). The following oligonucleotides were used for the qRT-PCR:

CYLD(Forward):5'-TGCCTTCCAACTCTCGTCTTG-3'

CYLD(Reverse): 5'-AAT CCG CTC TTC CCA GTA GG-3'

N-MYC(Forward):5'-AAGTAGAAGTCATCTTCGTCCGGGTAGAAGCAGGGCTGCA-3'

N-MYC(reverse): 5'-CGATTTCCTCCTCTTCATCTTCCTCCTCGTCATCCTCATC-3'

Apoptosis assay

Apoptosis was evaluated, using NucleoCounter NC-3000 (Chemometec), in conformity with the DNA fragmentation assay. Concisely: cells were grown on 6-well plates, harvested by trypsinization, and the trypsinized cells were pooled with the cells floating in the medium. After a short centrifugation, the supernatant was removed and the precipitated cells were washed once with PBS. After a second centrifugation, the cells were re-suspended in a small volume of PBS, and the single-cell suspensions were added to ice-cold 70% ethanol for fixation. Samples were vortexed and stored for 12-24 hours at -20°C. Ethanol-suspended cells were centrifuged and the ethanol carefully decanted. Cells were washed once with PBS and then re-suspended with

NucleoCounter Solution 3 (1 µg/ml DAPI, 0.1% Triton X-100 in PBS), followed by incubation for 5 minutes at 37°C. Samples of 10 µl volume were loaded into a slide chamber (NC-slide A8), and the DNA fragmentation protocol was employed according to the manufacturer's instructions (ChemoMetec).

NF-κB luciferase assay

The luciferase activity in cells transiently transfected with reporter constructs containing the kB promoter was determined using the Dual Luciferase Assay system (Promega). The luminescent signal was quantitated using the FLUOstar Optima plate reader (BMG Labtech). Luciferase expression was measured in cells transfected with plasmid constructs carrying the firefly luciferase reporter gene. As an internal control, plasmid pGL4.73 (Promega), containing the Renilla luciferase reporter gene, was co-transfected. The transfections were performed in Opti-MEM media containing 15 µl of Polyfect Transfection Reagent (Qiagen), and the cells were assayed for luciferase activity at 24 hours post-transfection, using reporter plasmids.

Immunofluorescence and confocal microscopy

Cells were washed in PBS, fixed with 4% paraformaldehyde in PBS for 4 minutes, washed twice in PBS and thereafter permeabilized and blocked with 5% goat serum or 5% bovine serum albumin and 0.3% Triton X-100 in PBS for 30 minutes. Cells were incubated with primary antibodies for 1 h. Following washes in PBS, cells were incubated with secondary Alexa Fluor 546- conjugated antibodies in PBS for 1 h followed by extensive washes in PBS and mounting on object slides using 20 µl PVA-DABCO (9.6% polyvinyl alcohol, 24% glycerol, and 2.5% 1,4-

diazabicyclo[2.2.2]octane in 67 mM Tris-HCl, pH 8.0). The images were obtained using a Zeiss LSM710 confocal microscope.

In vitro SUMOylation assay

1 μg of 6His-tagged CYLD purchased from Ubiquigent was used as a substrate for in vitro SUMOylation assay using a SUMOylation kit (Enzo Life Sciences) according to the manufacturer's instructions. Negative control reaction was carried out in the absence of ATP. After incubating the reaction for 1h at 30°C for, reaction was stopped by adding 2 x sample buffer. SUMOylation of protein was detected by immunoblotting using the anti-SUMO1 and anti-SUMO2/3 antibodies (Enzo Life Sciences).

In vitro deubiquitination assay

For in vitro deubiquitination assay, sumoylated and non-sumoylated CYLD were obtained by immunoprecipitation using the lysate prepared from SK-N-BE(2)C cells co-transfected with Flag, Flag-CYLD or Flag-CYLD K40R together with His-SUMO1. The immunoprecipitates were incubated with 200 ng/μl of poly-K63 ubiquitin in a reaction buffer (50 mM Tris-HCl, pH 7.5, 150 mM NaCl, 2 mM EDTA pH 8.0 and 2 mM dithiothreitol) in a total volume of 30 μl. The reactions were incubated for 2.5h at 37ºC and the reaction was terminated by adding SDS sample buffer including dithiothreitol. The reaction products were run on a SDS-PAGE gel followed by immunoblotting.

Pull-down assay

For the pull-down assay, Hela cells were grown in 6-well plates in the presence of 10% serum, containing DMEM-GlutaMAXTM-1. After reaching 80% confluence, the cells were transfected

with 2 μg of expression plasmids for 24 hours. The cells were lysed with buffer containing 50 mM Tris-HCl, 150 mM NaCl, 0.5 mM EDTA, and protease inhibitors. Equal amounts of cell lysate were used for the immunoprecipitation of Flag, using anti-Flag® M2 affinity gel (Sigma), TRAF2 (C-20, Santa Cruz), TRAF6 (H-274, Santa Cruz), HA (Y-11; Santa Cruz), SUMO1 (PW9460, Enzo Life Sciences), or SUMO2/3 (ab3742, Abcam) antibodies and incubated overnight at 4°C. The samples were centrifuged for 5 sec at 10,000 x g, and the supernatants were discarded. The pellets were washed three times with lysis buffer and the protein concentration was measured in the resulting supernatants. Equal amounts of protein and Ni-NTA magnetic agarose beads (Qiagen) for His pull-down, Flag-peptide for Flag pull down, or protein A/G for pulling down antibodies were added to the mixture, incubated for 2 hours at 4 °C and centrifuged for 5 sec at 10,000 x g. The bead complexes were collected and denatured for 5 min at 100 °C, followed by 2 min centrifugation at 12,000 x g. The supernatants were separated using SDS-PAGE and transferred onto PVDF membranes.

Statistical analyses

Statistical analyses were performed using GraphPad Prism5 Software (GraphPad Software, San Diego, CA, USA). Results are expressed as mean ± s.e.m., or as percent. P-values <0.05 were deemed statistically significant. Comparisons between groups were made using the Mann-Whitney U test. A correlation analysis was performed by determining the Pearson product-moment correlation coefficient.

Conflict of Interest

The authors declare no conflict of interest.

References

1.	Wagner LM, Danks MK. New therapeutic targets for the treatment of high-risk neuroblastoma. Journal of Cellular Biochemistry. 2009;107(1):46-57.

2.	Maris JM. Recent advances in neuroblastoma. The New England journal of medicine. 2010;362(23):2202-11. Epub 2010/06/19.

3.	Maris JM. Recent advances in neuroblastoma. The New England journal of medicine. 2010;362(23):2202-11. Epub 2010/06/19.

4.	Brodeur GM. Neuroblastoma: biological insights into a clinical enigma. Nature reviews Cancer. 2003;3(3):203-16. Epub 2003/03/04.

5.	Anderson DJ, Axel R. A bipotential neuroendocrine precursor whose choice of cell fate is determined by NGF and glucocorticoids. Cell. 1986;47(6):1079-90. Epub 1986/12/26.

6.	Anderson DJ, Carnahan JF, Michelsohn A, Patterson PH. Antibody markers identify a common progenitor to sympathetic neurons and chromaffin cells in vivo and reveal the timing of commitment to neuronal differentiation in the sympathoadrenal lineage. The Journal of neuroscience : the official journal of the Society for Neuroscience. 1991;11(11):3507-19. Epub 1991/11/01.

7.	Fredlund E, Ringner M, Maris JM, Pahlman S. High Myc pathway activity and low stage of neuronal differentiation associate with poor outcome in neuroblastoma. Proceedings of the National Academy of Sciences of the United States of America. 2008;105(37):14094-9. Epub 2008/09/11.

8.	Kogner P, Barbany G, Dominici C, Castello MA, Raschella G, Persson H. Coexpression of messenger RNA for TRK protooncogene and low affinity nerve growth factor receptor in neuroblastoma with favorable prognosis. Cancer research. 1993;53(9):2044-50. Epub 1993/05/01.

9.	Maris JM, Hogarty MD, Bagatell R, Cohn SL. Neuroblastoma. Lancet. 2007;369(9579):2106-20. Epub 2007/06/26.

10.	Matthay KK, Villablanca JG, Seeger RC, Stram DO, Harris RE, Ramsay NK, et al. Treatment of High-Risk Neuroblastoma with Intensive Chemotherapy, Radiotherapy, Autologous Bone Marrow Transplantation, and 13-cis-Retinoic Acid. New England Journal of Medicine. 1999;341(16):1165-73.

11.	Matthay KK, Reynolds CP, Seeger RC, Shimada H, Adkins ES, Haas-Kogan D, et al. Long-Term Results for Children With High-Risk Neuroblastoma Treated on a Randomized Trial of Myeloablative Therapy Followed by 13-cis-Retinoic Acid: A Children's Oncology Group Study. Journal of Clinical Oncology. 2009;27(7):1007-13.

12.	Sidell N, Altman A, Haussler MR, Seeger RC. Effects of retinoic acid (RA) on the growth and phenotypic expression of several human neuroblastoma cell lines. Experimental Cell Research. 1983;148(1):21-30.

13.	Pahlman S, Ruusala AI, Abrahamsson L, Mattsson ME, Esscher T. Retinoic acid-induced differentiation of cultured human neuroblastoma cells: a comparison with phorbolester-induced differentiation. Cell differentiation. 1984;14(2):135-44. Epub 1984/06/01.

14.	Ortoft E, Pahlman S, Andersson G, Parrow V, Betsholtz C, Hammerling U. Human GAP-43 Gene Expression: Multiple Start Sites for Initiation of Transcription in Differentiating Human Neuroblastoma Cells. Molecular and cellular neurosciences. 1993;4(6):549-61. Epub 1993/12/01.

15.   Kaplan DR, Matsumoto K, Lucarelli E, Thiele CJ. Induction of TrkB by retinoic acid mediates biologic responsiveness to BDNF and differentiation of human neuroblastoma cells. Eukaryotic Signal Transduction Group. Neuron. 1993;11(2):321-31. Epub 1993/08/01.

16.   Thiele CJ, Reynolds CP, Israel MA. Decreased expression of N-myc precedes retinoic acid-induced morphological differentiation of human neuroblastoma. Nature. 1985;313(6001):404-6.

17.   Clagett-Dame M, McNeill EM, Muley PD. Role of all-trans retinoic acid in neurite outgrowth and axonal elongation. Journal of Neurobiology. 2006;66(7):739-56.

18.   Bignell GR, Warren W, Seal S, Takahashi M, Rapley E, Barfoot R, et al. Identification of the familial cylindromatosis tumour-suppressor gene. Nat Genet. 2000;25(2):160-5.

19.   Massoumi R. CYLD: a deubiquitination enzyme with multiple roles in cancer. Future oncology. 2011;7(2):285-97. Epub 2011/02/25.

20.   Komander D, Lord CJ, Scheel H, Swift S, Hofmann K, Ashworth A, et al. The Structure of the CYLD USP Domain Explains Its Specificity for Lys63-Linked Polyubiquitin and Reveals a B Box Module. Molecular Cell. 2008;29(4):451-64.

21.   Komander D, Reyes-Turcu F, Licchesi JD, Odenwaelder P, Wilkinson KD, Barford D. Molecular discrimination of structurally equivalent Lys 63-linked and linear polyubiquitin chains. EMBO reports. 2009;10(5):466-73. Epub 2009/04/18.

22.   Trompouki E, Hatzivassiliou E, Tsichritzis T, Farmer H, Ashworth A, Mosialos G. CYLD is a deubiquitinating enzyme that negatively regulates NF-κB activation by TNFR family members. Nature. 2003;424(6950):793-6.

23.   Massoumi R, Chmielarska K, Hennecke K, Pfeifer A, Fassler R. Cyld inhibits tumor cell proliferation by blocking Bcl-3-dependent NF-kappaB signaling. Cell. 2006;125(4):665-77.

24.   Kovalenko A, Chable-Bessia C, Cantarella G, Israel A, Wallach D, Courtois G. The tumour suppressor CYLD negatively regulates NF-[kappa]B signalling by deubiquitination. Nature. 2003;424(6950):801-5.

25.   Brummelkamp TR, Nijman SM, Dirac AM, Bernards R. Loss of the cylindromatosis tumour suppressor inhibits apoptosis by activating NF-kappaB. Nature. 2003;424(6950):797-801. Epub 2003/08/15.

26.   Molenaar JJ, Koster J, Zwijnenburg DA, van Sluis P, Valentijn LJ, van der Ploeg I, et al. Sequencing of neuroblastoma identifies chromothripsis and defects in neuritogenesis genes. Nature. 2012;483(7391):589-93.

27.   Kohl NE, Gee CE, Alt FW. Activated expression of the N-myc gene in human neuroblastomas and related tumors. Science. 1984;226(4680):1335-7. Epub 1984/12/14.

28.   Seeger RC, Brodeur GM, Sather H, Dalton A, Siegel SE, Wong KY, et al. Association of Multiple Copies of the N-myc Oncogene with Rapid Progression of Neuroblastomas. New England Journal of Medicine. 1985;313(18):1111-6.

29.   Westermark UK, Wilhelm M, Frenzel A, Henriksson MA. The MYCN oncogene and differentiation in neuroblastoma. Seminars in Cancer Biology. 2011;21(4):256-66.

30.   Feng Z, Porter AG. NF-κB/Rel Proteins Are Required for Neuronal Differentiation of SH-SY5Y Neuroblastoma Cells. Journal of Biological Chemistry. 1999;274(43):30341-4.

31.   Kiningham KK, Cardozo Z-A, Cook C, Cole MP, Stewart JC, Tassone M, et al. All-trans-retinoic acid induces manganese superoxide dismutase in human neuroblastoma through NF-κB. Free Radical Biology and Medicine. 2008;44(8):1610-6.

32.	Bryan B, Kumar V, Stafford LJ, Cai Y, Wu G, Liu M. GEFT, A Rho Family Guanine Nucleotide Exchange Factor, Regulates Neurite Outgrowth and Dendritic Spine Formation. Journal of Biological Chemistry. 2004;279(44):45824-32.

33.	Liu T-X, Zhang J-W, Tao J, Zhang R-B, Zhang Q-H, Zhao C-J, et al. Gene expression networks underlying retinoic acid–induced differentiation of acute promyelocytic leukemia cells. Blood. 2000;96(4):1496-504.

34.	Deyrieux AF, Rosas-Acosta G, Ozbun MA, Wilson VG. Sumoylation dynamics during keratinocyte differentiation. Journal of Cell Science. 2007;120(1):125-36.

35.	Cheung NK, Dyer MA. Neuroblastoma: developmental biology, cancer genomics and immunotherapy. Nature reviews Cancer. 2013;13(6):397-411. Epub 2013/05/25.

36.	Bauters TG, Laureys G, Van de Velde V, Benoit Y, Robays H. Practical implications for the administration of 13-cis retinoic acid in pediatric oncology. International journal of clinical pharmacy. 2011;33(4):597-8. Epub 2011/05/06.

37.	Deng L, Wang C, Spencer E, Yang L, Braun A, You J, et al. Activation of the IκB Kinase Complex by TRAF6 Requires a Dimeric Ubiquitin-Conjugating Enzyme Complex and a Unique Polyubiquitin Chain. Cell. 2000;103(2):351-61.

38.	Chen J, Chen ZJ. Regulation of NF-κB by ubiquitination. Current Opinion in Immunology. 2013;25(1):4-12.

39.	Lovat PE, Irving H, Annicchiarico-Petruzzelli M, Bernassola F, Malcolm AJ, Pearson AD, et al. Apoptosis of N-type neuroblastoma cells after differentiation with 9-cis-retinoic acid and subsequent washout. Journal of the National Cancer Institute. 1997;89(6):446-52. Epub 1997/03/19.

40.	Celay J, Blanco I, Lazcoz P, Rotinen M, Castresana JS, Encio I. Changes in gene expression profiling of apoptotic genes in neuroblastoma cell lines upon retinoic acid treatment. PloS one. 2013;8(5):e62771. Epub 2013/05/08.

41.	O'Donnell MA, Perez-Jimenez E, Oberst A, Ng A, Massoumi R, Xavier R, et al. Caspase 8 inhibits programmed necrosis by processing CYLD. Nat Cell Biol. 2011;advance online publication.

42.	Wright A, Reiley WW, Chang M, Jin W, Lee AJ, Zhang M, et al. Regulation of early wave of germ cell apoptosis and spermatogenesis by deubiquitinating enzyme CYLD. Developmental cell. 2007;13(5):705-16. Epub 2007/11/06.

43.	Lee Moon H, Mabb Angela M, Gill Grace B, Yeh Edward TH, Miyamoto S. NF-κB Induction of the SUMO Protease SENP2: A Negative Feedback Loop to Attenuate Cell Survival Response to Genotoxic Stress. Molecular Cell. 2011;43(2):180-91.

44.	Wilkinson KA, Nakamura Y, Henley JM. Targets and consequences of protein SUMOylation in neurons. Brain Research Reviews. 2010;64(1):195-212.

Figure legends

Figure 1. High CYLD expression is associated with better overall survival and is relapse-free in neuroblastoma

(A-B) Kaplan-Meier survival curves for overall survival (A) and relapse-free survival (B) from 88 neuroblastoma patients (Versteeg-88-MAS5.0-u133p2) according to CYLD expression level (high or low) using the R2 microarray analysis and visualization platform (http://r2.amc.nl). Most significant expression cutoff value was used and p-value between two groups was calculated using a log rank test.

(C) Box and whiskers plot of CYLD mRNA expression in 61 neuroblastoma patients correlated with the International Neuroblastoma Staging System (INSS) that were derived from the R2 microarray analysis and visualization platform (http://r2.amc.nl).

(D) Box and whiskers plot of CYLD mRNA expression grouped according to N-MYC non-amplified and N-MYC amplified expression in 88 neuroblastoma patient samples using the R2 microarray analysis.

(E-F) The levels of CYLD RNA and protein in six different neuroblastoma cell lines. (+) indicates drug-resistance, and (-) indicates sensitive to drug treatment.

Figure 2. All-trans retinoic acid (ATRA) induces CYLD expression during neuroblastoma differentiation

(A) Phase-contrast microscopy images of SK-N-BE(2)C cells treated with medium, DMSO or 5 µM ATRA for 6 days. In another set of experiments SK-N-BE(2)C cells were treated with ATRA for 3 days and ATRA was replaced with DMSO for an additional 3 days (ATRA → DMSO). Lower panel shows neurite outgrowth in cells at high magnification.

(B) The expression of N-MYC at the mRNA level in SK-N-BE(2)C cells treated with 5 μM ATRA or DMSO for 2 or 3 days using quantitative RT-PCR.

(C) The levels of IκB-α in total cell lysates of SK-N-BE(2)C cells untreated or treated with 5 μM ATRA for 3 or 6 days. In another set of experiments SK-N-BE(2)C cells were treated with ATRA for 3 days and ATRA was replaced with DMSO for an additional 3 days.

(D-E) NF-κB luciferase promoter activity in SK-N-BE(2)C cells untreated or treated with 5 μM ATRA for different time points as indicated (*p<0.05).

(F) Percentage of apoptotic cells in SK-N-BE(2)C cells untreated or treated with 5 μM ATRA for 3, 6, 8 or 10 days using NucleoCounter NC-3000 (Chemometec) in conformity with the DNA fragmentation assay (*p<0.05).

Figure 3. Post-translational modification of CYLD induced by all-trans retinoic acid (ATRA) treatment in neuroblastoma cells

(A) CYLD gene expression using quantitative RT-PCR in SK-N-BE(2)C cells in the presence of medium, DMSO or 5 μM ATRA for 0, 1, 2, 3 and 6 days. In another set of experiments, cells were treated with ATRA for 3 days and ATRA was replaced with DMSO for an additional 3 days.

(B-C) Analysis of CYLD protein expression in untreated, ATRA-treated or SK-N-BE(2)C cells treated with ATRA for 3 days and replaced with DMSO for additional 3 days. Arrowhead indicates additional slow migrating band in ATRA treated cells.

(D) The levels of SUMO1 and SUMO2/3 in SK-N-BE(2)C cells untreated or treated with 5 μM ATRA for 3 and 6 days, or in cells where ATRA was replaced with DMSO for 3 days.

(E) Endogenous immunoprecipitation of CYLD in total cell lysates from ATRA (5 μM) treated (3 or 6 days) SK-N-BE(2)C cells, and a Western Blot, using CYLD or SUMO1 antibodies.

(F) Endogenous immunoprecipitation of SUMO1 or SUMO2/3 in 8M urea treated cell lysates from untreated or ATRA (5 µM for 3 days) treated SK-N-BE(2)C cells, and a Western Blot, using CYLD antibodies.

(G) Endogenous immunoprecipitation of SUMO1 in 8M urea treated cell lysates from untreated or ATRA (5 µM for 3, 6, 8 and 10 days) treated SK-N-BE(2)C cells, and a Western Blot, using CYLD antibodies. Lower panel shows post-translational modification of CYLD in total cell lysate of ATRA treated SK-N-BE(2)C cells. Arrowhead indicates additional slow migrating band in ATRA treated cells.

Figure 4. Identification of a SUMO conjugation motif at the N-terminal site of CYLD protein

(A) Purified GST-CYLD was used as substrate to perform the in vitro SUMOylation assay containing the E1, E2, E3, and SUMO1. Samples were immunoblotted with anti-GST, anti-SUMO1 and anti-SUMO2/3 antibodies.

(B) Immunoprecipitation of Flag in total Hela cell lysates transfected with Flag-tagged full length CYLD and His-tagged SUMO1, followed by a Western Blot, using Flag or His antibodies.

(C) GST-pull down assay using GST-tagged short fragment of CYLD (GST-CYLD-1-222) and His-tagged SUMO1 or His-tagged SUMO2. Samples were immunoblotted with anti-GST or anti-pan SUMO antibodies.

(D) Immunoprecipitation assay using Flag in Hela cells transfected with Flag-tagged short fragment of wildtype CYLD (Flag-CYLD-1-222) or Flag-tagged short fragment of CYLD SUMO mutant (Flag-CYLD-K40R) and His-SUMO1 expression constructs.

(F) Immunoprecipation assay using HA in Hela cells transfected with HA-tagged full length CYLD constructs (wildtype or mutant), His-SUMO1 or His-SUMO2 expression constructs, followed by a Western Blot, using HA or His antibodies.

Figure 5. CYLD SUMOylation reduces its deubiquitinase activity

(A) Western Blot analysis of Flag-tagged full length CYLD constructs (wildtype or mutant) in the absence or presence of MG132 in SK-N-BE(2)C cells transfected with ubiquitin K48R, full length or CYLD mutant constructs.

(B) Localization of CYLD (green) and α-Tubulin (red) in SK-N-BE(2)C cells transfected with EGFP, EGFP-CYLD wildtype or EGFP-CYLD K40R, using confocal immunofluorescence microscopy. DAPI (Blue) was used for nuclear staining.

(C) Immunoprecipation assay using Flag in SK-N-BE(2)C cells transfected with Flag-tagged full length CYLD (wildtype or mutant) and His-SUMO1 constructs followed by a Western Blot, using Flag, TRAF2 or TRAF6 antibodies.

(D) In vitro deubiquitination assay using ubiquitin conjugation kit (Boston Biochemistry) and addition of purified full length or SUMO mutant CYLD in the presence of purified SUMO1.

(E-F) Immunoprecipitation of endogenous TRAF6 in SK-N-BE(2)C cells transfected with wildtype or SUMO deficient CYLD, His-SUMO1, His-SUMO2, and Ubiquitin K48R constructs, followed by a Western Blot, using Flag, K63-Ubiquitin or TRAF6 antibodies.

(G) Immunoprecipitation of endogenous TRAF2 or TRAF6 in SK-N-BE(2)C cells transfected with Flag tagged CYLD (wildtype and mutant), Myc-SUMO1, and Ubiquitin constructs, followed by a Western Blot, using K63-Ubiquitin, TRAF2 or TRAF6 antibodies.

(H) Analysis of TRAF2 ubiquitination in Hela cells transfected with Flag-tagged TRAF2, ubiquitin, wildtype and SUMO mutant CYLD constructs.

(I) NF-κB luciferase activity in SK-N-BE(2)C cells untreated or treated with 5 μM ATRA for one day after transfection with wildtype or CYLD mutant expression constructs. (mean ± SEM, n=3, *p<0.05).

(J) Western Blot analysis of total levels of IκB-α, total p65, and phospho-p65 (recognizes serine 536) in SK-N-BE(2)C cells untreated or treated with 5 μM ATRA for one day after transfection with wildtype or SUMO mutant CYLD constructs.

(K) The morphological effects of the overexpression of CYLD or CYLD-K40R in SK-N-BE(2) cells in the presence of ATRA by counting the number of transfected cells with cell processes longer than the length of two cell bodies as an indication of differentiation. (mean ± SEM, n=3, *p<0.05).

(L) Model of ATRA-mediated regulation of NF-κB signaling by CYLD in neuroblastoma cells. SUMOylation of CYLD induced by ATRA inhibits DUB activity of CYLD and prevents removal of lysine 63 linked polyubiquitin chain from TRAF2 and TRAF6. This leads to activation of NF-κB signaling and differentiation of neuroblastoma cells. Prolonged ATRA treatment leads to reduced CYLD SUMOylation, which in turn, prevents activation of NF-κB signaling via deubiquitination of TRAF2/6 and facilitates cell death.
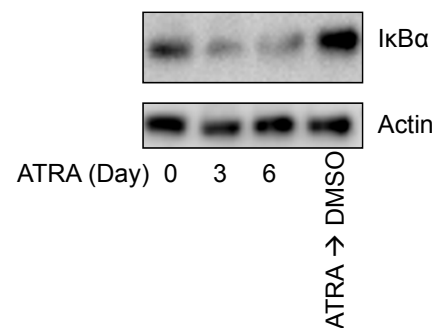
Figure 6. Correlation between CYLD and neural crest markers or late differentiation markers

(A) Correlation between CYLD and sympathetic neuronal differentiation marker genes (neurotrophic tyrosine kinase receptor type 1 (*NTRK1*) and growth associated protein 43 (*GAP43*)) were analyzed by calculating the Pearson's correlation coefficient using 88

neuroblastoma patients data extracted from the R2 microarray analysis and visualization platform (http://r2.amc.nl). Statistical analysis was carried out using two-sided unpaired t test.

(B) Correlation between CYLD and the early neural crest associated genes (vimentin (*VIM*) and inhibitor of DNA binding 2 (*ID2*)) were analyzed by calculating the Pearson's correlation coefficient using 88 neuroblastoma patients data extracted from the R2 microarray analysis and visualization platform (http://r2.amc.nl). Statistical analysis was carried out using two-sided unpaired t test.

Table 1

Correlation between CYLD and neural crest markers or sympatheric neuronal differentiation markers

Sympathetic neuronal differentiation markers	P-value	R	Gene ID
NTRK1(TrkA)	< 0.0001	0.455	4914
GAP43	< 0.0001	0.448	2596
NPY	0.0012	0.339	4852
STMN2 (SCG10)	0.00027	0.38	11075
BCL2	0.02	0.248	596

Early neuronal differentiation markers	P-value	R	Gene ID
VIM	0.003	-0.309	7431
ID2	0.04	-0.222	3398
MEIS1	0.19	0.14	4211
MEIS2	0.45	0.082	4212
KIT	0.05	0.21	3815

Correlation between CYLD and sympathetic neuronal differentiation marker genes or CYLD and the early neural crest associated genes were analyzed by calculating the Pearson's correlation coefficient using 88 neuroblastoma patients data extracted from the R2 microarray analysis and visualization platform (http://r2.amc.nl). Statistical analysis was carried out using two-sided unpaired t test. NTRK1: Neurotrophic tyrosine kinase, receptor, type 1, GAP43: growth associated protein 43, NPY: neuropeptide Y, STMN2: stathmin-like 2, BCL2: B-cell CLL/lymphoma 2, VIM: vimentin, ID2: inhibitor of DNA binding 2, MEIS1: Meis homeobox 1, MEIS2: Meis homeobox 2, KIT: v-kit Hardy-Zuckerman 4 feline sarcoma viral oncogene homolog.

[1]

Figure 1

Figure 2

Figure 3

Figure 4

A

DMSO | MG132

Flag-FL-CYLD + - + -
Flag-FL-CYLD (K40R) - + - +
Ub-K63R + + + +

130
100
IP: Flag
WB: Flag-CYLD

170
130
100
70
IP. Flag
WB: Ub

Lysate: α-Tubulin

B

DAPI | EGFP | Merge

EGFP

EGFP-FL-CYLD

EGFP-FL-CYLD (K40R)

C

Flag + - -
Flag-FL-CYLD - + -
Flag-FL-CYLD (K40R) - - +
His-SUMO1 + + +

TRAF2
TRAF6   IP: Flag
Flag-CYLD

Flag
TRAF6   Lysate
TRAF2

D

Poly-K63Ub + + +
Flag + - -
Flag-CYLD - + -
Flag-CYLD (K40R) - - +
His-SUMO1 + + +

80
70
50
40
30
25
15
Ub

140
115
80
Flag-CYLD

E

Flag + - -
Flag-FL-CYLD - + -
Flag-FL-CYLD (K40R) - - +
UbK48R + + +
His-SUMO1 + + +

IP: TRAF6
WB: Ub-K63

IP: TRAF6
WB: TRAF6

IP: TRAF6
WB: Flag

Lysate: Flag

Lysate: TRAF6

F

Flag + - -
Flag-FL-CYLD - + -
Flag-FL-CYLD (K40R) - - +
UbK48R + + +
His-SUMO2 + + +

IP: TRAF6
WB: Ub-K63

IP: TRAF6
WB: TRAF6

IP: TRAF6
WB: Flag

Lysate: Flag

Lysate: TRAF6

Figure 5

G

IP: | TRAF2 | IgG | TRAF6

Flag	+	-	-	+	+	-	-
Flag-FL-CYLD	-	+	-	-	-	+	-
Flag-FL-CYLD (K40R)	-	-	+	-	-	-	+
Ub-K48R	+	+	+	+	+	+	+
Myc-SUMO1	+	+	+	+	+	+	+

Ub

TRAF6
IgG   } IP
TRAF2

Lysate: Flag-CYLD

Lysate: TRAF6

Lysate: TRAF2

H

FLAG-TRAF2	-	+	+	+	+	+	+
HA-FL-CYLD	-	-	-	+	+	-	-
HA-FL-CYLD (K40R)	-	-	-	-	-	+	+
Ub-K48R	+	+	+	+	+	+	+
His-SUMO1	+	-	+	+	-	+	-

IP: FLAG-TRAF2
WB: Ub-K63

IP: FLAG-TRAF2
WB: FLAG

Lysate: FLAG-TRAF2

1 2 3 4 5 6 7

I

NF-κB luciferase activity (DLR ratio)

DMSO	+	-	-	-
ATRA	-	+	+	+
	Flag	Flag	Flag-FL-CYLD	Flag-FL-CYLD (K40R)

*

J

p-p65

p65

IκB-α

Actin

DMSO	+	-	-	-
ATRA	-	+	+	+
	Flag	Flag	Flag-FL-CYLD	Flag-FL-CYLD (K40R)

K

% transfected cells with long neurites

EGFP   EGFP-CYLD   EGFP-CYLDK40R

*

L

RA

TRAF2/6   CYLD → CYLD-S   TRAF2/6 U U U 63

IκB-α   IκB-α
NF-κB   U U U 48 NF-κB

NF-κB

CELL DEATH   CELL DIFFERENTIATION

Figure 5

A

NTRK (2 log of gene expression) vs CYLD (2 log of gene expression)
p < 0.0001
R = 0.4553

GAP43 (2 log of gene expression) vs CYLD (2 log of gene expression)
p < 0.0001
R = 0.448

B

VIM (2 log of gene expression) vs CYLD (2 log of gene expression)
p = 0.0034
R = - 0.3089

ID2 (2 log of gene expression) vs CYLD (2 log of gene expression)
p = 0.0375
R = - 0.2221

Figure 6
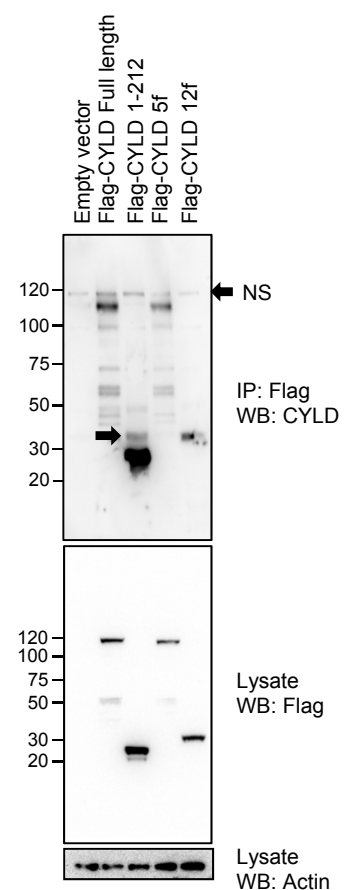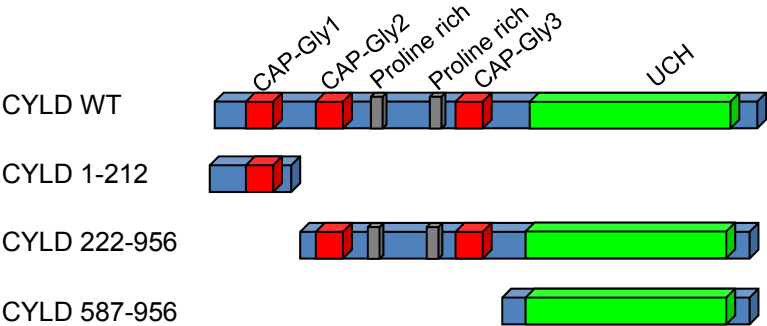
Supplementary Figure 1

Immunoprecipitation assay, using Flag in Hela cells transfected with Flag tagged full length CYLD or deletion of mutants of CYLD (CYLD 1-212, CYLD 222-956, or CYLD 587-956) and His tagged SUMO1, followed by a Western Blot, using Flag antibodies. Arrowhead shows a slower migrating band of CYLD 1-212. NS: nonspecific band.

Supplemental Figure 2

$$L\mathbf{R}_{VP}$$

↑

```
  1    MSSGLWSQEKVTSPYWEERIFYLLLQECSVTDKQTQKL L K VP KGSIGQYI
 51    QDRSVGHSRVPSTKGKKNQIGLKILEQPHAVLFVDEKDVVEINEKFTELL
151    LAITNCEERLSLFRNRLRLSKGLQVDVGSPVKVQLRSGEEKFPGVVRFRG
201    PLLAERTVSGIF
```

Supplementary Fig 2

The sequence of short fragment of CYLD (a.a. 1-212), where the motif with high probability for sumoylation is shown in red. Mutation of lyine 40 to arginine is shown in blue.
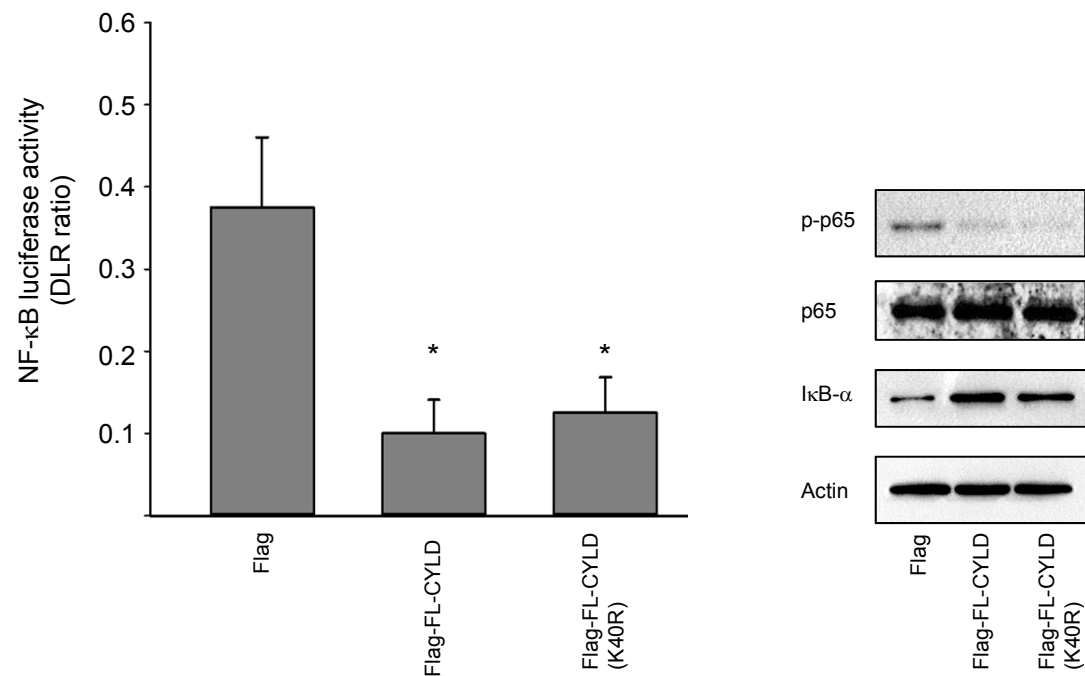
Supplemental Figure 3

Human	QKLLKVPKGS
Mouse	QKLLKVPKGS
Rat	QKLLKVPKGS
Chicken	QKLLKVPKGS
Chimpanzee	QKLLKVPKGS
Bovine	QKLLKVPKGS

Supplementary Fig 3

The sequence of CYLD protein SUMO binding site, which is highly conserved in many species including human, mouse, rat, chicken, chimpanzee, and bovine.
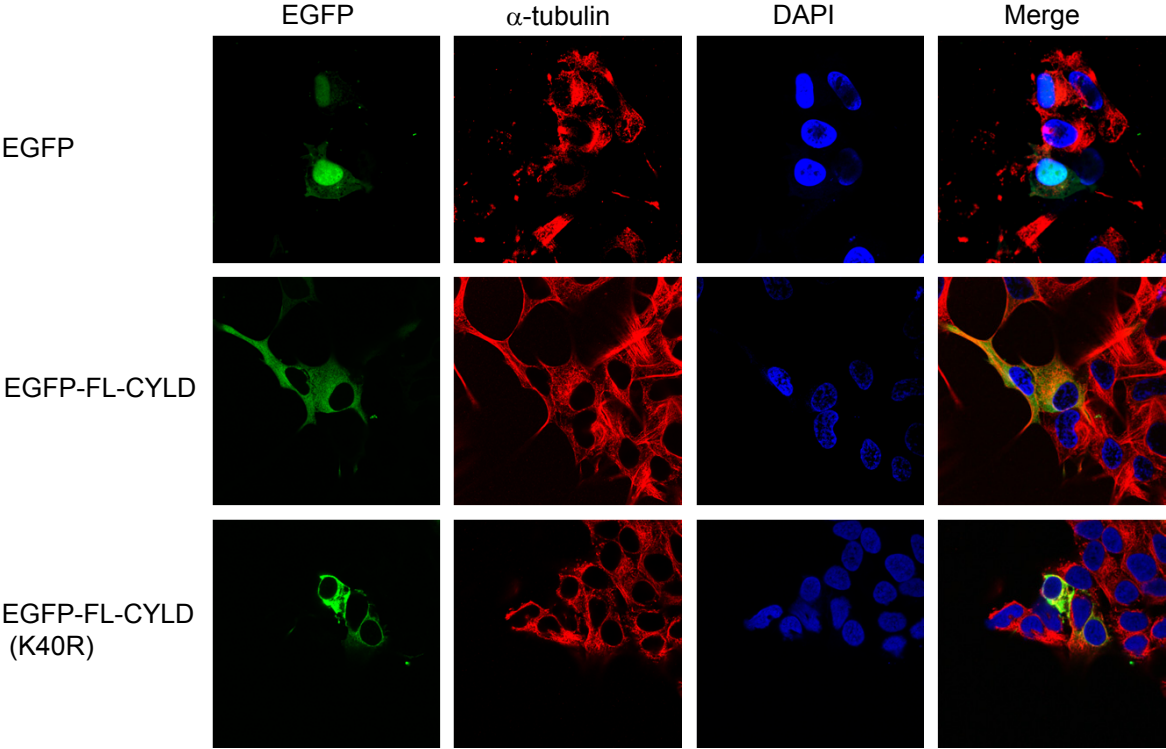
Supplemental Figure 4

Supplementary Figure 4

(Left panel) NF-kB luciferase activity in SK-N-BE(2)C cells after transfection with Flag, wildtype (Flag-FL-CYLD), or SUMO mutant CYLD (Flag-FL-CYLD-K40R) constructs (mean ± SEM, n=3, *p<0.05).

(Right panel) Western Blot analysis of total levels of IκB-α, phospho-p65, and p65 in SK-N-BE(2)C cells after transfection with Flag, wildtype (Flag-FL-CYLD), or SUMO mutant CYLD (Flag-FL-CYLD-K40R) constructs.

Supplemental Figure 5

	EGFP	α-tubulin	DAPI	Merge
EGFP				
EGFP-FL-CYLD				
EGFP-FL-CYLD (K40R)				

Supplementary Figure 5

The morphological effects of the overexpression of EGFP-CYLD or EGFP-CYLD-K40R in SK-N-BE(2) cells. Cells were washed in PBS, fixed with 4% paraformaldehyde in PBS for 4 minutes, washed twice in PBS and thereafter permeabilized and blocked with 5% goat serum or 5% bovine serum albumin and 0.3% Triton X-100 in PBS for 30 minutes. Cells were incubated with primary antibodies against α-tubulin (red) for 1 h. Following washes in PBS, cells were incubated with secondary Alexa Fluor 546- conjugated antibodies in PBS for 1 h followed by extensive washes in PBS and mounting on object slides using 20 μl PVA-DABCO. The images were obtained using a Zeiss LSM710 confocal microscope.